SCIENCE CHINA
Physics, Mechanics & Astronomy

• Review •
Special Topic: Optomechanics

May 2015 Vol. 58 No. 5: 050303
doi: 10.1007/s11433-015-5651-1

Hybrid opto-mechanical systems with nitrogen-vacancy centers

YIN ZhangQi[1*], ZHAO Nan[2,3*] & LI TongCang[4,5*]

[1]*Center for Quantum Information, Institute for Interdisciplinary Information Sciences, Tsinghua University, Beijing 100084, China;*
[2]*Beijing Computational Science Research Center, Beijing 100084, China;*
[3]*Synergetic Innovation Center of Quantum Information and Quantum Physics, University of Science and Technology of China, Hefei 230026, China;*
[4]*Department of Physics and Astronomy and School of Electrical and Computer Engineering, Purdue University, West Lafayette, IN 47907, USA;*
[5]*Birck Nanotechnology Center, Purdue University, West Lafayette, IN 47907, USA*

Received December 30, 2014; accepted January 21, 2015; published online February 6, 2015

In this review, we briefly review recent works on hybrid (nano) opto-mechanical systems that contain both mechanical oscillators and diamond nitrogen-vacancy (NV) centers. We also review two different types of mechanical oscillators. The first one is a clamped mechanical oscillator, such as a cantilever, with a fixed frequency. The second one is an optically trapped nano-diamond with a built-in nitrogen-vacancy center. By coupling mechanical resonators with electron spins, we can use the spins to control the motion of mechanical oscillators. For the first setup, we discuss two different coupling mechanisms, which are magnetic coupling and strain induced coupling. We summarize their applications such as cooling the mechanical oscillator, generating entanglements between NV centers, squeezing spin ensembles etc. For the second setup, we discuss how to generate quantum superposition states with magnetic coupling, and realize matter wave interferometer. We will also review its applications as ultra-sensitive mass spectrometer. Finally, we discuss new coupling mechanisms and applications of the field.

opto-mechanics, nitrogen-vacancy center, hybrid system

PACS number(s): 07.10.Cm, 42.50.wk, 37.10.Vz, 43.35.Gk, 63.20.kp

Citation: Yin Z Q, Zhao N, Li T C. Hybrid opto-mechanical systems with nitrogen-vacancy centers. Sci China-Phys Mech Astron, 2015, 58: 050303, doi: 10.1007/s11433-015-5651-1

1 Introduction

In 2012, David Wineland, together with Serge Haroche, won the Nobel prize "for ground-breaking experimental methods that enable measuring and manipulation of individual quantum systems" (The Nobel Prize in Physics 2012). In Wineland's lab, the motion and the electron spin of trapped ions couple with each other. Therefore, the motional degree of freedom of the trapped ions can be coherently manipulated, such as the ground state cooling, Fock states generating and detecting with unit fidelity and efficiency [1]. Using these technologies, David Wineland generated Shrödinger's cat states with trapped ions [2, 3], which for many years only existed in thought experiment.

The "true" Shrödinger's cat state is defined by a microscopic two-level system entangling with a macroscopic system. New technology, such as opto-mechanics, is needed to generate quantum superpositions in macroscopic systems. Opto-mechanics involves the study of the radiation pressure on the mechanical oscillator, and how to use this pressure to manipulate the motion of mechanical systems. In the 17th century Kepler found the radiation pressure of light when he studied the comet tails. In 1909, Einstein [4] studied the statistics of radiation pressure force fluctuations on a movable mirror. In the 1960s, Braginsky [5] studied the role of radiation pressure in the context of interferometers, and proposed to cool the motionnal temperature of the mirror by radiation

*Corresponding author (YIN ZhangQi, email: yinzhangqi@ mail.tsinghua.edu.cn; ZHAO Nan, email: nzhao@csrc.ac.cn; LI TongCang, email: tcli@purdue.edu)

pressure. In 1969, Ashkin [6] observed optical trapping of micron-sized particles in liquid. Two years later, optical levitation of glass spheres by an upward-propagating laser beam in both air and vacuum was demonstrated [7]. The optical tweezers are now widely used in atomic physics, chemistry, and biology.

Recent years, we have witnessed great developments of opto-mechanics [8–10]. Quantum ground state of macroscopic mechanical oscillators was achieved by traditional cryogenic techniques in 2010 [11], or by active cooling in 2011 [12, 13]. Many technologies based on opto-mechanics have been developed. For example, Verhagen et al. [14] have transferred the signals from light to mechanical oscillation, and vise versa. Weis et al. [15–17] have realized optomechanically induced transparency, and Purdy et al. [18] have generated squeezed lights in opto-mechanical systems. By using mechanical oscillator as an interface, quantum information has been able to exchange between microwave superconducting circuits and optical lights [19–21].

In the future, the aim is to achieve a similar controlling ability in macroscopic resonators as Monroe, et al. did in the trapped ions [3]. Then Schrödinger's cat states with macroscopic objects [22], or even macroscopic living objects, such as viruses [23] can be generated. As macroscopic quantum superposition states become bigger and bigger, it could be possible to identify the intrinsic decoherence mechanisms such as gravity induced decoherence [24], Continuous Spontaneous Localization models [25, 26], and etc.. More information on the theory and development of optomechanics can be found in these reviews [8–10,27].

In order to generate the non-classical states in an opto-mechanical oscillator, strongly quadratic coupling between the oscillator and the optical mode is essential [22]. However, it is usually very challenging to get a large quadratic coupling in experiments. Inspired by the trapped ion experiments, the quadratic coupling can be replaced by coupling the mechanical oscillator to a two-level quantum system, which can be externally controlled well. In order to get the stable macroscopic quantum states, the coherence time of both the mechanical oscillator and the spin 1/2 should be maximized. There are several proposals that are based on quantum dots [28, 29], atoms [30], superconducting qubits [11], and nitrogen-vacancy centers (NV centers) [31–34]. Among all these proposals, the ones with NV centers are most attractive. As NV centers have presented the coherence even at room temperature.

NV centers in diamonds are usually regarded as artificial atoms in solid systems. The diamond lattice consists of covalently bound carbon atoms, which makes diamonds very stiff. The valence electrons in diamond have huge bandgap (5.48 eV), which makes it transparent deep into the UV. In its lattice, nitrogen and vacancy are the most common defects. As shown in Figure 1, an NV center consists of a nitrogen atom and a vacancy at the nearest neighboring site. The NV centers are usually negatively charged, possessing 6 electrons and

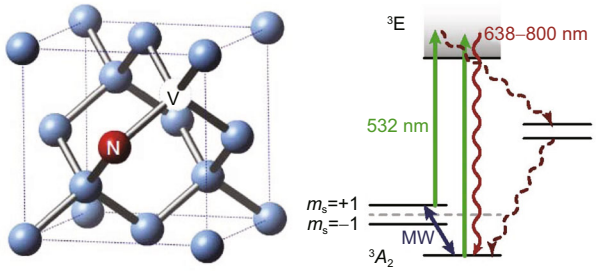

Figure 1 (Color online) The figure in the left shows lattice structure of diamond with nitrogen-vacancy center. The image in the right shows the negatively charged NV center electronic energy level structure. Electronic spin polarization and readout is performed by optical excitation at 532 nm and red fluorescence detection around 637 nm. Ground-state spin manipulation is achieved by resonant microwave excitation. The ground-state triplet has a zero magnetic field splitting $\simeq$ 2.87 GHz. Figure adopted from ref. [35]. Copyright (2012) by Nature Publishing Group.

spin $S = 1$ in the ground state.

NV centers are promising candidate system for quantum information processing. Single NV centers can be addressed using the confocal microscopy technique. The spin state of the NV centers can be initialized and read-out at room temperature, respectively, by optical pumping and spin-dependent fluorescence. Furthermore, the spin state manipulation can be achieved by resonant microwave radiation. Because of the weak spin-orbital coupling of the diamond material, and low concentration of ^{13}C, the only spin-carrying isotope of carbon with natural abundance 1.1%, electron spin of NV centers in diamond has very long coherence time ($\sim$ ms) even at room temperature [36]. All these properties mentioned above make NV centers excellent candidates for quantum logic elements for quantum information processing.

In addition to the applications in quantum information, NV centers are widely used as solid-state ultra sensitive magnetic field sensor. Again, because of the long coherence time, even a tiny change in the magnetic field can be monitored by measuring its effect on the spin dynamics of NV centers. Recent experiments demonstrated high sensitivity $\sim$ nT/$\sqrt{\text{Hz}}$ at atomic scale resolution [37, 38]. Furthermore, recent research shows that, not only magnetic fields, other types of signal (e.g., electric fields, temperature, and strain etc.) which can be converted to magnetic signal can also be precisely measured by NV center spins. This makes NV centers very amazing multi-functional atomic-scale sensors.

There are two methods to interface the NV centers and the mechanical oscillators. The first one is based on strong magnetic field gradient to couple the mechanical oscillators with NV centers [31]. The second one requires the strain induced effective electric field to mix phonon mode with NV centers electron spins [39]. A strong coupling can be achieved in both of the methods. Once the strong coupling regime is achieved, we may cooling the mechanical oscillator with coherent excitation exchange between spin and motion degrees [31, 40]. We can generate arbitrary superposition states of mechanical oscillator. We may realize phonon laser and squeezing in the

system [39,41]. The system can also be used for the quantum information processing [32], as it can interface many different degrees of freedom.

To increase the coherence time of the mechanical oscillator, we can optimize the design and choose the materials with high mechanical Q, such as Si_3N_4 with Q around 10^6 [42]. However, the best way is optically trapping the nanodiamond in vacuum [23,43–51]. The mechanical Q factor in this system could be as high as 10^{10}, which is comparable to the trapped ions. It is possible to cool the trapped nanoparticle from room temperature [52]. Another advantage is that the strong coupling between the oscillation and the spin can be realized with a modest magnetic field gradient around 10^5 T/m. It is also possible to couple the rotation degree of freedom to the spins. Besides, the trapping frequency can be easily tuned, even completely turned off, which makes the time-of-flight measurement possible [53].

In an optical trap, the motion of a nano-particle can be cooled to mK by feedback without cavity [44, 45]. Ground state may be reached by means of cavity sideband cooling [46, 47], or by exchanging excitations between phonon and spin degrees [31, 53, 54]. Even at thermal states, matter wave interference could be observed in this systems [53, 55, 56]. By detecting the coherence of NV center spin, the ultrasensitive mass spectrometer is realizable even at room temperature [57].

2 Nanomechanical cantilevers coupled with NV centers

To couple NV center electron spins with a mechanical resonator, we need to apply additional magnetic field gradient, or induce a strain in the lattice of diamonds. Here we will briefly discuss these two different methods, and illustrate several applications for both of the methods.

2.1 Magnetic field gradient induced coupling

2.1.1 The setup

The idea of strong magnetic coupling between a mechanical oscillator and a NV center is shown in Figure 2 [31]. Here a single NV center electron spin is used for sensing the motion of the mechanical oscillator. It should be noted that the NV center can also be attached to the end of the resonator [33], other than the magnetic tip shown in Figure 2. The frequency of the mechanical oscillator is ω_r. The oscillation induces a time-varying magnetic field, which causes Zeeman shifts of the electron spin. The single phonon induces frequency shift $\lambda = g_s\mu_b G_m a_0$, where $g_s \simeq 2$, μ_B is Bohr magneton, G_m is the magnetic field gradient, and $a_0 = \sqrt{\hbar/2m\omega_r}$ is the zero field fluctuation for a resonator of mass m. We will show that in the current experiments, λ can be as high as 100 kHz, which is larger than both the spin coherence time (1 ms), and the damping rate $\gamma = \omega_r/Q$ of high Q mechanical resonators.

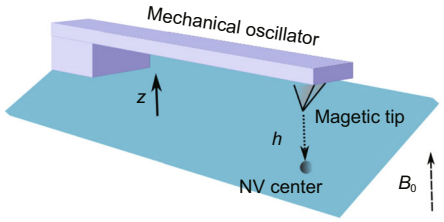

Figure 2 (Color online) A magnetic tip, which is attached to the end of a cantilever, is placed at a distance h above a single NV center. It creates a strong magnetic gradient near the electronic spin of the NV center. As the spin energy is in proportional to the magnetic field, a strong coupling between the NV center electron spin and the motion of cantilever is created. Laser field is used for initializing and measuring the spin states. Microwave is used for manipulating the the spin states.

The Hamiltonian of the system can be written as:

$$H_S = H_{NV} + \hbar\omega_r a^\dagger a + \hbar\lambda(a + a^\dagger)S_z, \tag{1}$$

where H_{NV} describes the dynamics of NV center electron spin, $a(a^\dagger)$ is the annihilation (creation) operator of the phonon in the mechanical oscillator, and S_z is the z component of the spin-1 operator of NV center. We assume that the NV sysmetry axis is also aligned along z direction. The NV center electron spin ground state is an $S = 1$ triplet. The three states are labled as $|0\rangle, |\pm 1\rangle$. Without external magnetic field, the levels $|\pm 1\rangle$ are degenerate. The zero field splitting between $|0\rangle$ and $|\pm 1\rangle$ is $\omega_0/2\pi = 2.88$ GHz. In order to manipulate the levels $|\pm 1\rangle$ individually, we add a static magnetic field B_0 along z axis to break the degenerate states $|\pm 1\rangle$. The frequencies difference between $|0\rangle$ and $|\pm 1\rangle$ are $\omega_{\pm 1} = \omega_0 \pm \mu_B B_0/\hbar$.

In order to enable coherent exchange the excitation between the mechanical resonator and the spin, we need to add microwaves to drive Rabi oscillations between $|0\rangle$ and $|\pm 1\rangle$. We assume the magnetic field oscillation amplitudes is much less than $\hbar\omega_0/\mu_B$. In a rotating wave frame we have

$$H_{NV} = \sum_{i=\pm 1} -\hbar\Delta_i|i\rangle\langle i| + \frac{\hbar\Omega_i}{2}(|0\rangle\langle i| + |i\rangle\langle 0|), \tag{2}$$

where $\Delta_{\pm 1}$ and $\Omega_{\pm 1}$ denote the detunings and the Rabi frequencies of the two microwave transitions. For simplicity, we assume that $\Delta_{+1} = \Delta_{-1} = \Delta$ and $\Omega_{+1} = \Omega_{-1} = \Omega$. The eigenstates of N_{NV} are $|d\rangle = (|-1\rangle - |+1\rangle)/\sqrt{2}$, $|g\rangle = \cos\theta|0\rangle - \sin\theta|b\rangle$, and $|e\rangle = \cos\theta|b\rangle + \sin\theta|0\rangle$, where $|d\rangle = (|+1\rangle + |-1\rangle)\sqrt{2}$, and $\tan(2\theta) = -\sqrt{2}\Omega/\Delta$. The eigenvalues corresponding to are $\omega_d = -\Delta$, and $\omega_{e,g} = (-\Delta \pm \sqrt{\Delta^2 + 2\Omega^2})/2$. In the case that $\Delta < 0$, the lowest energy state is $|g\rangle$. We adjust the frequency difference between $|d\rangle$ and $|g\rangle$ $\omega_{dg} = \omega_d - \omega_g$ to be equal to the mechanical frequency ω_r, and the frequency difference between $|e\rangle$ and $|d\rangle$ $\omega_{ed} = \omega_e - \omega_d$ is largely detuned with ω_r. Under the condition $|\omega_r - \omega_{ed}| \gg \lambda$, we will have effective Jaynes-Cummings Hamiltonian

$$H_{JC} = \hbar\lambda_g|g\rangle\langle e|a^\dagger + \text{h.c.}, \tag{3}$$

where $\lambda_g = -\lambda \sin\theta$.

In this system, phonon-spin coupling strength λ is usually much less than phonon frequency ω_r, which is around 10 MHz. Therefore, it is impossible to directly generate Schrödinger's cat states in this setup. We will discuss how to realize a frequency tunable mechanical oscillator in the next section. By tuning the mechanical frequency less than λ, the Schorödinger's cat states in a macroscopic mechanical resonator can be prepared with spin-dependent force [53].

2.1.2 *Applications as resonator cooling*

With JC Hamiltonian eq. (3), we can coherently manipulate the mechanical states with the help of spin states if a strong coupling condition is fulfilled. The decay of a mechanical resonator at temperature T is defined as $\Gamma_r = k_B T/\hbar Q$. The spin dephasing rate is $\delta\omega_{dg}$. The strong coupling condition is $\lambda_g > \Gamma_r, \delta\omega_{dg}$. In experiments, we may use Si cantilever of dimensions $(l, w, t) = (3, 0.05, 0.05)$ μm with frequency $\omega_r = 7$ MHz and $a_0 = 5 \times 10^{-13}$ m. A magnetic tip can induce gradient field $G_m = 10^7$ T/m at the distant $h = 25$ nm. The phonon-spin coupling strength $\lambda = 100$ kHz is realizable. The mechanical Q can be as high as 10^5 and the heating rate is $\Gamma_r/2\pi = 20$ kHz. The spin decay can be around $\delta\omega_{gd} = 1$ kHz if we use a Carbon-13 purified diamond. Therefore, the strong coupling condition can be fulfilled.

To manipulate the phonon states of the resonator, the first step is to cool it to the ground state. If the mechanical oscillator frequency is high enough, e.g. > 1 GHz, we can use the traditional cryogenic techniques to cool the environment to 10 mK, and the resonator is already in its quantum ground state. Usually the resonator frequency is around MHz, we have to use an active method to cool it to ground state. In opto-mechanics, we need cavity mode as an vacuum bath to cool the mechanical mode. In this setup, we don't need a cavity, as the NV center can be used as an effective vacuum bath. By using JC Hamiltonian (3) and optical pump technology of NV center spin states, we can cool the resonator to the ground state. The basic idea is as follows. We initialize the NV center spin to $|0\rangle$ by using an optical pump in the time scale less than 1 μs. Then we use microwave to prepare the spin state to $|g\rangle$. By turning on the microwave driving we use JC Hamiltonian (3) to exchange transfer excitation from resonator to the NV center spin in the time scale $1/\lambda_g \sim 10$ μs. At last we initialize the NV center again. By repeating the process, the excitations in the resonator are quickly removed. Under the condition $\lambda_g > \Gamma_r$, a quantum ground state cooling should be possible. If we carefully adjust the detuning of the driving microwave and laser, the above procedure can be automatically repeated to cool the mechanical resonator [31].

The above cooling method is only valid for low temperature $T < 1$ K and mechanical frequency $\omega_r \sim 1$ MHz. For high temperature, the Lamb-Dicke (LD) limit is not fulfilled, the cooling with NV center spins is no longer possible [58], as shown in Figure 4. When thermal phonon phonon is larger than $N_{th}^c = 10^4$, the cooling effects quickly disappear. After preparation of quantum ground state, arbitrary superposition states of the resonator should be possible. However, to generate the high fidelity phonon states, we need a high Q resonator, which is very difficult for this system. We will discuss this problem in sect. 3.

2.1.3 *Applications in quantum information processing*

Once mechanical ground state is prepared, the mechanical resonator can be used for quantum information processing [59–61]. By charging the mechanical oscillator, distant coupling between resonators is also possible [32].

In order to entangle distant NV centers, we need to couple multiple NV centers to the same mechanical oscillator, which is used as a quantum bus. As shown in Figure 4, Xu et al. [60] considered a scheme where an array of a NV centers equidistant from each other, above which are one-to-one magnetic tips attached at the end of a cantilever. The qubits are encoded in two spins levels $|0\rangle$ and $|-1\rangle$. We applied a microwave to globally drive all the NV center spins. We assume that all NV center spins have the same transition frequency ω_0 and the frequency of microwave is on resonant with ω_0. We define the new basis for the spins as $|\pm\rangle = (|-1\rangle \pm |+1\rangle)/\sqrt{2}$. Consider the case that the Rabi frequency of microwave Ω is comparable to the mechanical frequency ω_r, in rotating wave approximation, we have the effective Hamiltonian of the system as:

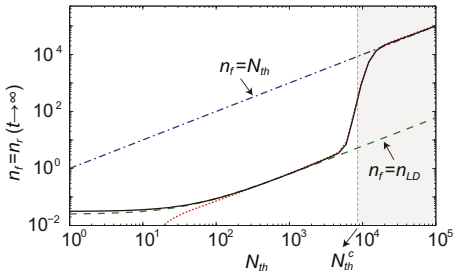

Figure 3 (Color online) Steady state phonon occupation number n_f as a function of the environment thermal excitation N_{th}. The value of N_{th}^c denotes the crossover from LD regime to a regime where phonon cooling is strongly suppressed and finally $n_f = N_{th}$. Firgure adopted from ref. [58]. Copyright (2010) by the American Physical Society.

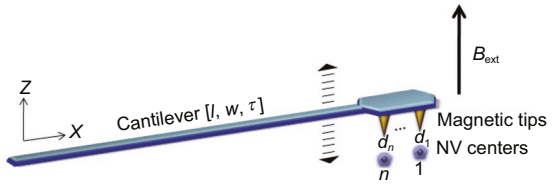

Figure 4 (Color online) A scheme to entangle multiple NV centers spins that couple with the same mechanical oscillator. An array of evenly spaced magnetic tips are attached at the end of a nanomechanical cantilever, under which are one-to-one correspondent NV centers. Figure adapted from ref. [60]. Copyright (2010) by the American Physical Society.

$$H_I = \sum_{j=1}^{n} \frac{\lambda}{2} a|+\rangle_j\langle -| \exp[-i\delta(t)dt] + \text{h.c.}, \tag{4}$$

with $\delta(t) = \omega_r - \Omega(t)$. The collective Hamiltonian eq. (4) can be used for generating W states. As an example, initially we prepare the phonon state to the Fock state $|1\rangle$ with phonon number 1, and the NV centers to the state $|-\rangle_1|-\rangle_2\cdots|-\rangle_n$. We set the detuning $\delta(t) = 0$, the W state $|W\rangle = (|+\rangle_1|-\rangle_2\cdots|-\rangle_n + |-\rangle_1|+\rangle_2\cdots|-\rangle_n\cdots|-\rangle_1|-\rangle_2\cdots|+\rangle_n)/\sqrt{n}$ can be generated at the time $t = \pi/(\sqrt{n}\lambda)$.

If the detuning $\delta(t)$ is much larger than coupling strength λ, it will induce the effective spin-spin coupling between NV centers [59, 62]. In ref. [59], they only considered two NV centers coupling with the same cantilever. Assume the detuning $\delta_1 = \delta_2 = \delta$, to the second order we have the effective Hamiltonian

$$H_{eff} = \frac{\hbar\lambda_g^2}{4\delta}\left[\left(a^\dagger a + \frac{1}{2}\right)(\sigma_{1z} + \sigma_{2z}) - (\sigma_{1+}\sigma_{2-} + \sigma_{1-}\sigma_{2+})\right]. \tag{5}$$

As we discussed in sect. 2.1.2, the phonon-spin coupling $\hbar\lambda$ could be around 100 kHz. In order to fulfill the condition $\delta \gg \lambda_g$, we choose $\hbar\delta$ in the order of 1 MHz. The spin-spin coupling $\hbar\lambda_g^2/(4\delta)$ is in the order of 10 kHz, which is larger than both NV center spin decoherence rate and the effective phonon decay rate at 10 mK temperature. Therefore, it is possible to generate the entanglement among NV centers spins in experiments with high fidelity.

The idea can be extended to realize a scalable quantum information processor [32]. As shown in Figure 5, the processor consist of an array of N nanomechanical resonators, each of which is coupled magnetically to an electronic spin qubit associated with an impurity located in the substrate below. As we discussed in sect. 2.1.2, the resulting spin-phonon coupling could be as high as 100 kHz under the magnetic gradient 10^7 T/m. The long range interaction between distant sites can be established by charging the resonator and capacitively coupling with the nearby wire. The Hamiltonian of the resonators is

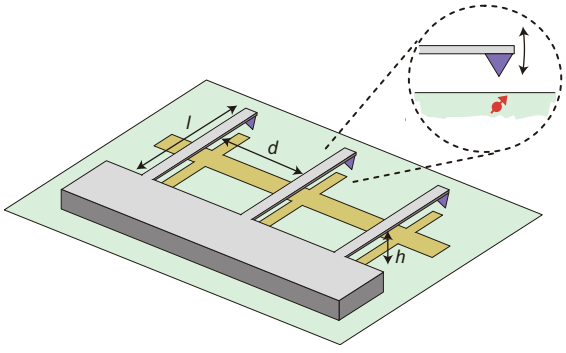

Figure 5 (Color online) Schematic view of a scalable quantum information processor on an electromechanical quantum bus and NV centers spins as qubits. Figure adapted from ref. [32]. Copyright (2010) by Nature Publishing Group.

$$\begin{aligned} H_{cr} &= \sum_i \hbar\omega_r a_i^\dagger a_i + \frac{\hbar}{2}\sum_{i,j} g_{ij}(a_i + a_i^\dagger)(a_j + a_j^\dagger) \\ &= \sum_n \hbar\omega_n a_n^\dagger a_n. \end{aligned} \tag{6}$$

After combining magnetic and electric coupling Hamiltonians, we have the full Hamiltonian of the system,

$$H_{cr} = H_s(t) + \hbar\sum_n \hbar\omega_n a_n^\dagger a_n + \frac{1}{2}\sum_{i,n}\lambda_{i,n}(a_n^\dagger + a_n)\sigma_z^i, \tag{7}$$

where $H_s(t) = \sum_i \hbar(\delta_i\sigma_z^i + \Omega_i(t)\sigma_x^i)/2$, ω_n and a_n denote frequencies and collective mode operators for phonon eigenmodes. This model is quite similar to the quantum computation proposal for trapped ions systems. However, here the decoherence mechanism and physical implementation are different. Anyway, the idea of using hybrid systems that contain mechanical resonators array and NV centers for quantum information processing needs to be further investigated in the future.

2.1.4 Applications in ultra-sensitive measurement

As the resonator is coupled with NV center spin, we can use the NV center as a detector to measure the state of resonator [33, 34]. Therefore, the NV center spin can be used as an ultra-sensitive detector for the mechanical resonators. Even though strong coupling conditions are not fulfilled, we may still detect the Brownian motion of the resonator in classical regime.

In ref. [33], a hybrid system in which a single nitrogen-vacancy center coupled with a nanomechanical oscillator is realized. As show in Figure 6, a single NV center hosted in a nano-diamond is placed at the extremity of a Sic nanowire. By adding a strong magnetic field gradient to the system, a magnetic coupling between NV center and mechanical oscillator is induced. The motion of nanowire can be probed by reading out a single electron spin of the NV center.

Ref. [34] reported the coherent coupling of a mechanical cantilever to the single spin of NV center. The authors used the electronic spin of an NV center to sense the motion of a magnetized cantilever. Although the change of the magnetic field due to the motion of the cantilever was very small, it could still be monitored by measuring the NV center spin coherence. This was achieved with the help of the spin echo technique, where the spin is flipped by microwave π pulses during the evolution. With this technique, the unwanted background noise is filtered out, while the signal to be detected (i.e., the magnetic field signal from the cantilever motion) is magnified. In ref. [34], the authors successfully demonstrated a motion sensing with precision down to $\sim$ pm under ambient conditions. Later, we will show that the spin-echo-based technique is not limit in motion sensing. Indeed, it can be applied in sensing various types of signals [57].

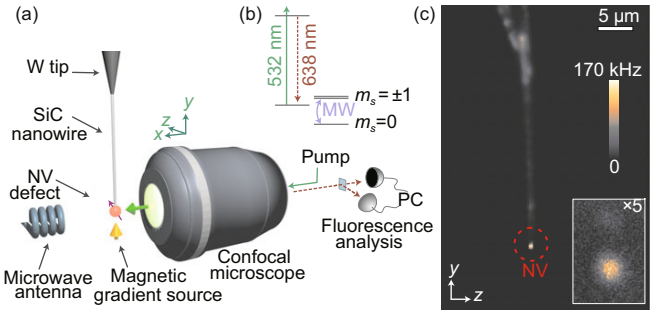

Figure 6 (Color online) (a) A confocal microscope monitors the fluorescence of a single NV defect hosted in a diamond nanocrystal placed at the extremity of a SiC nanowire. A microwave antenna is used to manipulate the NV electronic spin, while a micro-fabricated magnetic structure approaching in the vicinity of the suspended NV centre generates a strong magnetic field gradient. (b) The electronic levels structure of the NV centres at zero magnetic field. (c) Fluorescence map of the system recorded with the confocal microscope while scanning the objective position. The isolated bright spot circled in red corresponds to the fluorescence of a single NV centre. Inset: Enlarged view of the nanowire extremity. Figure adapted from ref. [33]. Copyright (2011) by Nature Publishing Group.

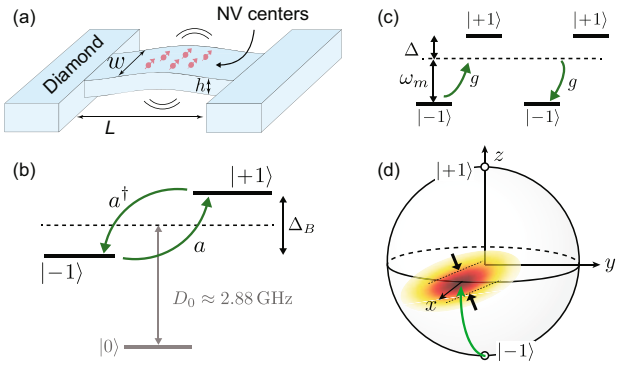

Figure 7 (Color online) (a) All-diamond doubly clamped mechanical resonator with an embedded NV centers ensemble (NVE). (b) Spin levels and transitions of NV centers electron spins. Local perpendicular strain induced by beam bending mixes the $|\pm 1\rangle$ states. (c) NV centers spins in the two-level subspace $|\pm 1\rangle$ off-resonantly couple with a common mechanical mode. (d) NVE collective spins squeezing. Figure adopted from ref. [39]. Copyright (2013) by The American Physical Society.

2.2 Strain induced coupling

2.2.1 Model

In the previous subsection, we summarized the recent works on hybrid systems with a mechanical resonator and a NV center, where a strong magnetic gradient induces spin-phonon coupling. In this section, we will review a new mechanism that couples NV center electrons and the phonon mode in diamond, strain induced spin-phonon coupling, and effective spin-spin interactions between NV centers, as proposed by ref. [39]. The spin-spin interactions can induce spin squeezing in NV center ensembles (NVE), which may be used in NVE magnetometry.

As shown in Figure 7(a), we considered an NVE embedded in a single crystal diamond nanobeam [39]. When the beam oscillates, it strains the lattice of the diamond, and induces direct coupling between NV center electrons spins and the mechanical mode. Here we write down the Hamiltonian for NV center, in the presence of external electric and magnetic fields $\boldsymbol{E}$ and $\boldsymbol{B}$ [39, 63]

$$\begin{aligned} H_{\rm NV} =&(D_0 + d_{\parallel}E_z)S_z^2 + \mu_B g_s \boldsymbol{S}\cdot\boldsymbol{B} \\ &- d_{\perp}[E_x(S_xS_y + S_yS_x) + E_x(S_x^2 - S_y^2)], \end{aligned} \tag{8}$$

where $D_0/2\pi = 2.88$ GHz is the zero field splitting, $g_s \simeq 2$, μ_B is the Bohr magneton, and $d_{\parallel}$ ($d_{\perp}$) is the ground state electric dipole moment in the direction parallel (Perpendicular) to the NV axis [64].

As shown in Figure 7(b), the motion of nanoresonator changes the local strain of the NV center, and induces an effective electric field. We are interested in the near resonant coupling between a single motion mode and $|\pm 1\rangle$ transition of the NV center. The Zeeman splitting between $|\pm 1\rangle$ is $\Delta_B = g_s\mu_B B_z/\hbar$. The perpendicular component of strain $E_{\perp}$ mixes $|\pm 1\rangle$ states with interaction Hamiltonian $E_{\perp} = E_0(a + a^\dagger)$, where a is the destruction operator of the resonator mode with frequency ω_m. E_0 is the zero point motion of the beam induced perpendicular strain. The parallel strain also induces the level shifts between $|\pm 1\rangle$ and $|0\rangle$. However, in the subspace $|\pm 1\rangle$ the parallel strain plays no role in the system, as state $|0r\rangle$ is not involved. In this subspace, the interaction Hamiltonian of each NV center is

$$H_I = \hbar g(a^\dagger\sigma_i^- + a\sigma_i^+), \tag{9}$$

where $\sigma_i^{\pm} = |\pm 1\rangle\langle\mp 1|$ is Pauli operator for ith NV center and g is the single phonon coupling strength. For NVE, we can define the collective spin operators, $J_z = \frac{1}{2}\sum_i |1\rangle_i\langle 1| - |-1\rangle_i\langle -1|$ and $J_{\pm} = J_x \pm iJ_y = \sum_i \sigma_i^{\pm}$. The total Hamiltonian is

$$H_T = \omega_m a^\dagger a + \Delta_B J_z + g(a^\dagger J_- + aJ_+). \tag{10}$$

Here for simplicity, we assume that coupling g is uniform for all NV centers. The interaction between NV centers is also neglected as we assume that they are far apart from each other.

The coupling strength g can be estimated with the following equation [39]

$$\frac{g}{2\pi} \approx 180\left(\frac{\hbar}{L^3 w\sqrt{\rho E}}\right)^{1/2}, \tag{11}$$

where ρ is the mass density and E is the Young's modulus of the diamond. Up to now, it is only achieved the single phonon coupling strength $g \sim 0.25$ Hz in a diamond resonator [65]. Theoretically, we may get $g \sim 1$ kHz in the future. For a beam of dimensions $(L, w, h) = (1, 0.1, 0.1)$ μm we got $\omega_m/2\pi \sim 1$ GHz and coupling $g/2\pi \sim 1$ kHz. We define the single spin cooperativity $\eta = g^2T_2/(\gamma\bar{n}_{th})$, where $\gamma = \omega_m/Q$ is the mechanical decay rate and T_2 is the spin dephasing time, and $\bar{n}_{th}$ is the thermal equilibrium phonon number for the resonator. It is found that η could be as high as 0.8 for $T = 4$ K, $T_2 = 10$ ms, and $Q = 10^6$. To get $\eta > 1$, we need to further decrease the dimension of the diamond resonator, or decrease

the temperature T. Similarly as sect. 2.1.2, the Hamiltonian can also be used for cooling the mechanical oscillator if the strong coupling condition is fulfilled [41].

2.2.2 *Spin squeezing*

Similarly as we discussed in sect. 2.1.3 [59, 62], in a large detuning limit that $g \ll \Delta = \Delta_B - \omega_m$, we can adiabatically eliminate the mechanical mode a, and get effective spin-spin interactions [39]. The effective Hamiltonian is

$$H_{eff} = \omega_m a^\dagger a + (\Delta_B + \lambda a^\dagger) J_z + \frac{\lambda}{2} J_+ J_-, \qquad (12)$$

where $\lambda = 2g^2/\Delta$. The Hamiltonian eq. (12) can be used for generating spin squeezing state. To generate the spin squeezed state, we initialized the NVE to coherent spin state $|\psi_0\rangle$ along x axis, which satisfies $J_x|\psi_0\rangle = J|\psi_0\rangle$. It has equal transverse variances $\langle J_x^2\rangle = \langle J_x^2\rangle = J/2$. The interaction term $J_+J_- = \boldsymbol{J}^2 - J_x^2 + J_z$, where total angular momentum J is conserved and J_z^2 induces spin variance squeezing in one direction, as shown in Figure 7(d). The squeezing can be qualified by the parameter

$$\xi^2 = \frac{2J\langle \Delta J_{\min}^2 \rangle}{\langle J_x \rangle^2}, \qquad (13)$$

where $\langle \Delta J_{\min}^2 \rangle = \frac{1}{2}(V_+ - \sqrt{V_-^2 + V_{yz}^2})$ is the minimum spin uncertainty with $V_\pm = \langle J_y^2 \pm J_z^2 \rangle$ and $V_{yz} = \langle J_y J_z + J_z J_y \rangle/2$. If we prepare the spin squeezed state with $\xi^2 < 1$, it has a direct applications for magnetometry of NVE below the projection noise limit [66].

In Figure 8(a), the squeezing parameter verse time is plotted for an ensemble of $N = 100$ spins and several $\bar{n}_{\rm th}$. The decoherence of spin and mechanical decay is also considered by solving master equation [39]. We plot the scaling of the squeezing parameter with J for small decoherence in Figure 8(b). It was found that the scalling is $\xi^2_{\rm opt} \sim J^{-2/3}$.

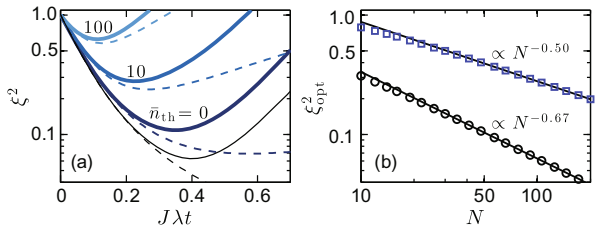

Figure 8 (Color online) (a) Spin squeezing parameter versus scaled precession time with $N = 100$ spins. Thick blue (gray) lines show the calculated squeezing parameter for $T_2 = 10$ ms and values of $\bar{n}_{\rm th}$ as shown. For each curve, the squeezing is optimized. Dashed lines are calculated from the linearized equations for the spin operator averages. (b) Optimal squeezing versus number of spins. Lower(upper) line shows power law fit for $\bar{n}_{\rm th} = 1(10)$ and $T_2 = 1(0.01)$s. Other parameters in both plots are $\omega_m = 1$ GHz, $g/2\pi = 1$ kHz, $Q = 10^6$. Figure adopted from ref. [39]. Copyright (2013) by the American Physical Society.

3 Optically trapped nano-diamond that hosts NV centers

As we stated in the introduction, one of the key factors affecting macroscopic Schrödinger's cat state is the mechanical Q factor. In this section we will focus on the optically trapped nanodiamond system, whose mechanical Q factor is not related to the material, but the pressure of the vacuum. For the current technology, we can assume Q to be high as 10^{10}. Therefore, the life time of Schrödinger's cat state can be as long as a millisecond.

3.1 Scheme and Fock states preparation

As shown in Figure 9(a), we consider a nano-diamond trapped by an optical tweezers in a high-Q cavity in vacuum. Therefore, the mechanical motion of the nano-diamond couples with the cavity mode. The trap is located in a place that the cavity mode has the maximum gradient. Near the NV center, there is a magnetic tip, which induces a strong magnetic field gradient. The magnetic gradient couples the mechanical motion and the electron spin. There is also a microwave source to control the spin of the NV center inside the nano-diamond. As the nano-diamond is optically trapped in vacuum, the coherence time of the mechanical mode for its center-of-mass motion is long [53]. The frequency of the optical trap can be quickly tuned through control of the laser intensity. This feature is important as we can cool the mechanical mode to the ground state in a strong trap and prepare large quantum superposition states of the nano-diamond in a weak trap by a quench of the trap frequency.

Once the resonator cooled down, we can generate many non-classical states, such as Fock states. The NV spin is initially set to the state $|0\rangle$, which is decoupled from the mechanical mode during the cooling. Initialization and single shot detection of the NV spin have been well accomplished experimentally [67]. We assume that the NV center is at a

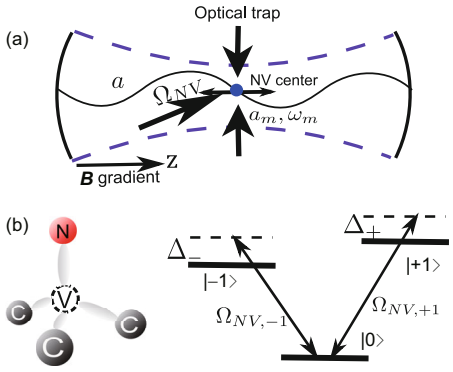

Figure 9 (Color online) (a) A nano-diamond with an NV center is optically trapped in vacuum with spin-mechanical coupling enabled through a nearby magnetic tip and opto-mechanical coupling through a cavity around. (b) The atomic structure (left) and the level diagram (right) in the ground state manifold for a NV center in the nanodiamond. Figure adopted from ref. [53]. Copyright (2013) by the American Physical Society.

position with zero magnetic field and a large field gradient. We apply a microwave drive with the Hamiltonian $H_{\rm drive} = \hbar(\Omega_{\rm NV,+1}e^{i\omega_{l+}t}|0\rangle\langle+1| + \Omega_{\rm NV,-1}e^{i\omega_{l-}t}|0\rangle\langle-1| + h.c.)/2$ and set the Rabi frequency $\Omega_{\rm NV,\pm1} = \Omega_{\rm NV}$ and the detuning $\Delta_\pm \equiv \omega_{l\pm} - \omega_{\pm1} = \Delta$. With $\Delta \gg |\Omega_{\rm NV}|$, we adiabatically eliminate the level $|0\rangle$ and get the following effective Hamiltonian

$$H_e = \hbar\omega_m a_m^\dagger a_m + \hbar\Omega\sigma_z + \hbar\lambda(\sigma_+ + \sigma_-)(a_m + a_m^\dagger), \quad (14)$$

where $\Omega = |\Omega_{\rm NV}|^2/4\Delta$, $\sigma_z = |+\rangle\langle+| - |-\rangle\langle-|$, $\sigma_+ = |+\rangle\langle-|$, $\sigma_- = |-\rangle\langle+|$, and we have defined the new basis states $|+\rangle = (|+1\rangle + |-1\rangle)/\sqrt{2}$, $|-\rangle = (|+1\rangle - |-1\rangle)/\sqrt{2}$. In the limit $\lambda \ll \omega_m$, we set $\Omega = \omega_m/2$ and use the rotating wave approximation to get an effective interaction Hamiltonian between the mechanical mode and the NV center spin, with the form

$$H_{JC} = \hbar\lambda\sigma_+ a_m + h.c..$$

This represents the standard Jaynes-Cummings (J-C) coupling Hamiltonian. Similarly, if we set $\Omega = -\omega_m/2$, the anti-J-C Hamiltonian can be realized with

$$H_{aJC} = \hbar\lambda\sigma_+ a_m^\dagger + h.c..$$

Arbitrary Fock states and their superpositions can be prepared with a combination of J-C and anti-J-C coupling Hamiltonians. For example, to generate the Fock state $|2\rangle_m$, we initialize the state to $|+\rangle|0\rangle_m$, turn on the J-C coupling for a duration $t_1 = \pi/(2\lambda)$ to get $|-\rangle|1\rangle_m$, and then turn on the anti-J-C coupling for a duration $t_2 = t_1/\sqrt{2}$ to get $|+\rangle|2\rangle_m$. The Fock state with an arbitrary phonon number n_m can be generated by repeating the above two basic steps, and the interaction time is $t_i = t_1/\sqrt{i}$ for the ith step. Superpositions of different Fock states can also be generated. For instance, if we initialize the state to $(c_0|+\rangle + c_1|-\rangle) \otimes |0\rangle_m/\sqrt{2}$ through a microwave with arbitrary coefficients c_0, c_1, and turn on the J-C coupling for a duration t_1, we get the superposition state $|-\rangle\otimes(c_1|0\rangle_m + ic_0|1\rangle_m)/\sqrt{2}$. Using the optical cavity, the Fock state $|n_m\rangle_m$ of mechanical mode can also be mapped to the corresponding Fock state of the output light field [46].

The effective QND Hamiltonian for the spin-phonon coupling takes the form

$$H_{QND} = \hbar\chi\sigma_z a_m^\dagger a_m,$$

with $\chi = 4\Omega\lambda^2/(4\Omega^2 - \omega_m^2)$ when the detuning $||\Omega| - \omega_m/2| \gg \lambda$. The Hamiltonian $H_{\rm QND}$ can be used for a quantum nondemolition measurement (QND) measurement of the phonon number: we prepare the NV center spin in a superposition state $|+\rangle + e^{i\phi}|-\rangle)/\sqrt{2}$, and the phase ϕ evolves by $\phi(t) = \phi_0 + 2\chi n_m t$, where $n_m = a_m^\dagger a_m$ denotes the phonon number. Through a measurement of the phase change, one can detect the phonon number.

Let us estimate the typical parameters. A large magnetic field gradient can be generated by moving the nano-diamond close to a magnetic tip. Though magnetic gradients up to 10^7 T/m have been realized [68, 69], here we take the gradient $G = 10^5$ T/m, which is much less than the one used in Sec. 2.1.2 [31]. We get the coupling $\lambda \simeq 2\pi\times52$ kHz for a nanodiamond with the diameter $d = 30$ nm in an optical trap with a trapping frequency $\omega_m = 2\pi\times0.5$ MHz. The QND detection rate $2|\chi| \sim 2\pi\times25$ kHz with the detuning $||\Omega| - \omega_m/2| \sim 5\lambda$. The NV electron spin dephasing time over 1.8 ms has been observed at room temperature [36], which is long compared with the Fock state preparation time $1/\lambda$ and the detection time $1/(2|\chi|)$.

3.2 Macrocopic quantum superpositions

To prepare spatial quantum superposition state, we need to generate quantum superposition of the nanodiamond at distinct locations. To detect the superposition state, we need to do interference experiment, either with matter wave [53] or with the spin [55].

3.2.1 Matter wave interference

Without the microwave driving, the spin-mechanical coupling Hamiltonian takes the form

$$H = \hbar\omega_m a_m^\dagger a_m + \hbar\lambda S_z(a_m + a_m^\dagger). \quad (15)$$

The mechanical mode is initialized to the vacuum state $|0\rangle_m$ (or a Fock state $|n_m\rangle_m$) in a strong trap with the trapping frequency ω_{m0} and the NV center spin is prepared in the state $|0\rangle$. Although the ground state cooling is most effective in a strong trap, to generate large spatial separation of the wave packets it is better to first lower the trap frequency by tuning the laser intensity for the optical trap. While it is possible to lower the trap frequency through an adiabatic sweep to keep the phonon state unchanged, a more effective way is to use a nonadiabatic state-preserving sweep [70], which allows arbitrarily short sweeping time. We denote $|n_m\rangle_{m1}$ as the mechanical state in the lower frequency ω_{m1}. We then apply an impulsive microwave pulse to suddenly change the NV spin to the state $(|+1\rangle + |-1\rangle)/\sqrt{2}$ and simultaneously decrease the trap frequency to $\omega_{m2} \leqslant \omega_{m1}$. The evolution of the system state under the Hamiltonian (15) then automatically splits the wave packet for the center-of-mass motion of the nano-diamond. The splitting attains the maximum at time $T_2/2 = \pi/\omega_{m2}$, where the maximum distance of the two wave packets in the superposition state is $D_m = 8\lambda a_2/\omega_{m2} = 4g_s\mu_B G/(m\omega_{m2}^2)$, where $a_2 = \sqrt{\hbar/2m\omega_{m2}}$. At this moment, the system state is

$$|\Psi_S\rangle = (|+1\rangle|D_m/2\rangle_{n_m} + |-1\rangle|-D_m/2\rangle_{n_m})/\sqrt{2}, \quad (16)$$

where $|\pm D_m/2\rangle_{n_m} \equiv (-1)^{a_m^\dagger a_m} e^{\pm D_m(a_m^\dagger - a_m)/4a_2}|n_m\rangle_1$ is the displaced Fock state (or coherent states when $n_m = 0$). This is just the entangled spatial superposition state.

The maximum distance D_m is plotted in Figure 10(a) versus trap frequency, magnetic field gradient, and diameter d of the nano-diamond, and superposition states with separation D_m comparable to or larger than the diameter d is achievable under realistic experimental conditions.

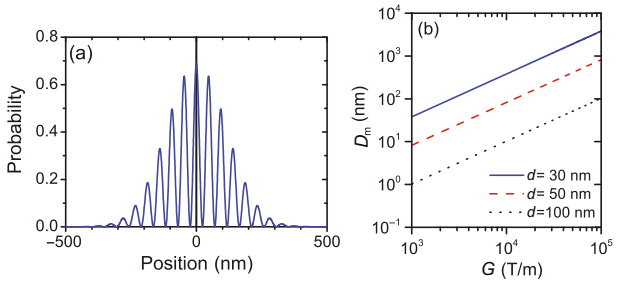

Figure 10 (Color online) (a) Spatial interference patterns for a 30 nm nano-diamond after 10 ms of free expansion. The nano-diamond is initially prepared in the vacuum state $|0\rangle_m$ or the 1-phonon state $|1\rangle_m$ of a 20 kHz trap. The magnetic gradient is 3×10^4 T/m. Before the trap is turned off, the center of mass of the nano-diamond is prepared in $|\psi_+\rangle_0$. (b) Maximum spatial separation D_m as a function of the magnetic gradient G when the trapping frequency is 1 kHz. Macroscopic superposition states with separation larger than the size of the particle can be achieved with a moderate magnetic gradient. Figure adopted from ref. [53]. Copyright (2013) by the American Physical Society.

To transform the entangled cat state $|\Psi_S\rangle$ to the standard cat state $|\psi_\pm\rangle_{n_m} \equiv (|D_m/2\rangle_{n_m} \pm |-D_m/2\rangle_{n_m})/\sqrt{2}$, we need to apply a disentangling operation to conditionally flip the NV spin using displacement of the diamond as the control qubit. This can be achieved as different displacements of the wavepacket induce relative energy shifts of the spin levels due to the applied magnetic field gradient [53]. To detect spatial superposition state, we can turn off the optical trap and let the spatial wave function freely evolve for some time t. The split wave packets will interference just like the Young's double slit experiment. The period of the interference pattern is $\Delta z = 2\pi\hbar t/(mD_m)$. As an estimation of typical parameters, we take $\omega_{m1} = \omega_{m2} = 2\pi \times 20$ kHz, $d = 30$ nm, and magnetic field gradient 3×10^4 T/m. The spin-phonon coupling rate $\lambda \simeq 2\pi \times 77$ kHz and the maximum distance $D_m \simeq 31a_2$. The preparing time of the superposition state is about 25 μs, which is much less than the coherence time of the NV spin. For the time of flight measurement after turn-off of the trap, we see the interference pattern with a period of 47 nm after $t = 10$ ms, as shown in Figure 10, which is large enough to be spatially resolved [44, 45].

3.2.2 Ramsey interference

The challenge of matter wave interference proposal is that the mass and velocity varies for an ensemble of nano-diamonds [55]. In order to overcome this challenge, ref. [55] proposed to used Ramsay interferometry to observe the interference. With Ramsay interence, we can verify the matter wave superpositions, as well as the quantum contextuality for macroscopic quantum systems [56]. The basic setup of their poposal is the same as Figure 9. Here we assume that an angle θ between the vertical and the z axis of the system. The Hamiltonian of the system is

$$H = \hbar D S_z^2 + \hbar\omega_r a_m^\dagger a_m - 2\hbar(\lambda S_z - \Delta\lambda)(a_m + a_m^\dagger), \quad (17)$$

where $D = 2.87$ GHz is the zero field splitting, and $\Delta\lambda = \frac{1}{2}mg\cos\theta\sqrt{\frac{\hbar}{2m\omega_r}}$. Let's denote $\mu = 2(S_z\lambda - \Delta\lambda)/\hbar\omega_r$. The initial state of resonator is a coherent state $|\beta\rangle$. The spin dependent time evolution of the state is $|\beta(t, S_z)\rangle|S_z\rangle$, where $S_z = 0, \pm 1$. We get that

$$\beta(t, S_z)\rangle = \mathrm{e}^{-\mathrm{i}(D-\omega_r\mu^2)t+\mathrm{i}\mu^2\sin(\omega_r t)}|(\beta-\mu)\mathrm{e}^{-\mathrm{i}\omega_r t} + \mu\rangle.$$

A striking feature of this evolution is that the oscillator returns to its original coherent state β for any β and S_z at time $t_0 = 2\pi/\omega_r$.

As an example, we consider an initial separable state $|\beta\rangle|S_z\rangle$. By using a strong microwave pulse $H_{mw} = \hbar\Omega(|+1\rangle\langle 0| + |-1\rangle\langle 0| + \text{h.c.}$, we can change the state to $|\Psi(0)\rangle = \beta\rangle(|+1\rangle + |-1\rangle)/\sqrt{2}$. The state after an oscillation period $t_0 = 2\pi/\omega_r$ becomes

$$|\Psi(t_0)\rangle = |\beta\rangle\left(\frac{|+1\rangle + \mathrm{e}^{\mathrm{i}\Delta\phi_g}|-1\rangle}{\sqrt{2}}\right), \quad (18)$$

where we have $\Delta\phi_g = 16\lambda\Delta\lambda t_0/(\hbar^2\omega_r)$. We apply microwave Hamiltonian H_{mw} again to transfer the spin population to $|0\rangle$. After time $t_p = \pi/(2\sqrt{2}\Omega)$, we get

$$P_0 = \cos^2\left(\frac{\Delta\phi_g}{2}\right),$$

which can be used to measure the relative phase $\Delta\phi_g$. The detection of $\Delta\phi_g$ is an evidence for the matter wave superposition state. Besides, as the phase $\Delta\phi_g$ is not dependent on the initial state β, it is possible to be observed when the initial state is thermal.

3.3 Applications as mass spectrometer

As mentioned above, one of the most attractive features of the system of optically levitated particles is its high mechanical quality factor. The trapped particle can coherently oscillate many times (e.g., 10^{10} times) before its mechanical energy damps out. When this kind of almost-perfect mechanical oscillator couples to a long-live quantum object, i.e. NV center electron spin, fantastic quantum phenomena and a novel application can be expected.

In ref. [57], we studied the quantum dynamics of a coupled system of a quantum oscillator and a single spin, where the spin is under dynamical decoupling control. Dynamical decoupling control, as an extended version of spin echo technique, has been proved to be an efficient method to prolong the spin coherence time. In ref. [57] we predicted that, under dynamical decoupling control and coupled to a high-quality mechanical oscillator, the spin coherence will exhibit a series of periodic peaks, forming a comb structure (called time-comb in ref. [57]). The peak width is calculated as:

$$\Delta_{q^*} \equiv \frac{2\sqrt{2}}{\gamma_{q^*}} = \frac{T_0}{N\Lambda\sqrt{2n_{\mathrm{th}}+1}}. \quad (19)$$

Two features are notable in the above equation. First, the peak width is inversely proportional to the square root of the thermal occupation number n_{th} of the mechanical oscillator,

which implies narrower peaks in higher temperature. Second, the peak width is inversely proportional to the control pulse number N. Since the control pulse number N is related to the total coherent evolution time, and the later can be regarded as a kind of resource in high-precision sensing, we expected that improving the dynamical decoupling control pulse number can improve the measurement sensitivity.

Based on the time-comb structure, we propose an ultra-sensitive mass spectrometer using the coupled qubit-oscillator system. Since the peak position in the time axis is synchronized with oscillator period, we propose to infer the oscillator period (and its mass assuming a constant spring coefficient) by measuring the peak position. Obviously according to the error propagation formula, the narrower the peak is, the better sensitivity we will have. The two features mentioned above make the proposed mass spectrometer different to those based on traditional measurement principles. As the peak will be narrower in higher temperatures, we propose that the mass spectrometer will have a counterintuitive temperature dependence on the sensitivity (i.e., higher temperature helps improve the sensitivity). This result makes the room-temperature application of ultra-sensitive mass spectrometer possible. The second feature, as we showed in ref. [57], implies an improved scaling of the measurement sensitivity to the measurement resource. The scaling relation goes beyond the shot-noise scaling and Heisenberg scaling in the quantum metrology theory. The underlying physics that brings about this improved scaling is under further research.

3.4 Experimental progresses

Dielectric nanoparticles have been trapped and cooled optically, as shown in refs. [44, 45, 47]. Following a similar method, trapping a nano-diamond in atmosphere pressure has been realized experimentally in 2013 [54]. The experimental setup is shown in Figure 12. They found evidence of NV photoluminescence from a nano-diamond in a free-space optical dipole trap. The photoluminescence rates are decreased with increasing trap laser power. The neutral charge state (NV^0) can be suppressed by a continuous-wave trap.

The charged nano-diamond was also levitated in a linear quadrupole ion trap in air under ambient conditions [71]. An electric trap has no trapping laser that quenches fluorescence emission. The surface charge has effects on the emission rates of fluorescence spectrum of NV center. However, there is no difference in the spectral property found in the experiment. Up to now, there is no report on trapping nano-diamond in vacuum. This is the first problem that should be overcome in future experiments.

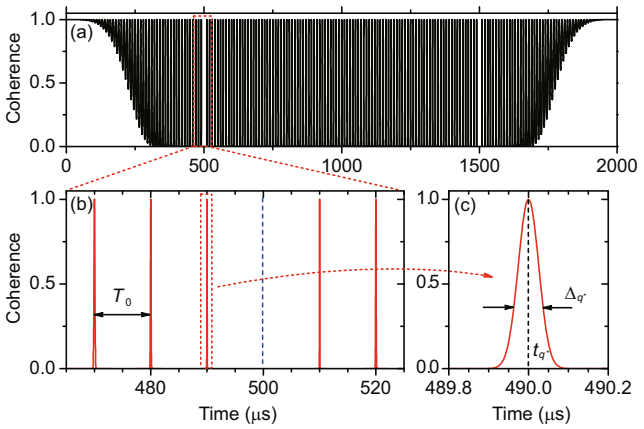

Figure 11 (Color online) (a) The time-comb structure of qubit coherence under 100-pulse CPMG control. For $\omega_r t \gg 1$, the comb period is synchronized with the oscillator period $T_0 = 2\pi/\omega_r$. (b) Close-up of the coherence peaks. A missing peak at $\omega_r t = N\pi$ is indicated by the blue dashed line. The peak width is decreasing when getting close to the missing one. (c) Close-up of the narrowest coherence peak, which is centered at t_{q^*} with width Δ_{q^*} (see text). The parameters used in this figure are oscillator frequency 100 kHz, coupling strength $\lambda = 0.0001\omega_r$, temperature $T = 10$ K, and 100-pulse CPMG control. Figure adopted from ref. [57]. Copyright (2014) by the American Physical Society.

4 Conclusion and outlook

In this paper, we gave a brief review on the field of (opto)nano-mechanical resonator coupling with NV centers electrons spins. We discussed magnetic and strain induced phonon-spin coupling mechanisms. We discussed how to cool the resonator to the ground state and how to manipulate the phonon non-classical states. We also discussed how to realize quantum information processing in this system. We reviewed the progresses in an optically trapped nano-diamond with building in NV centers. We discussed how to observe macroscopic quantum interference in the system. We also discussed how to used the system as an ultra-sensitive mass spectrometer at room temperature. Finally, we briefly summarized the experimental progresses.

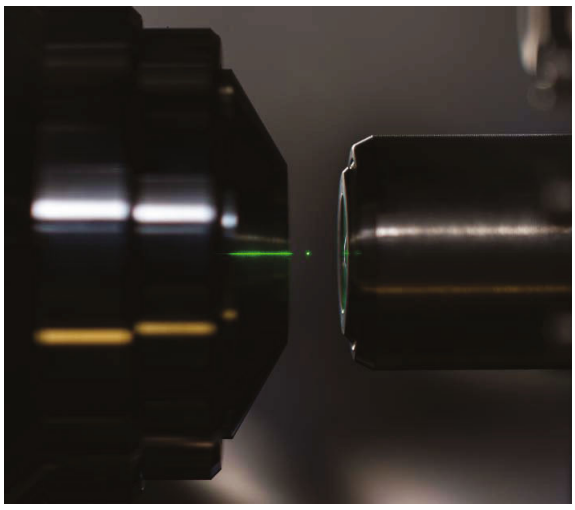

Figure 12 (Color online) A photograph of a ~ 100 nm diameter nano-diamond, which is levitated by an optical tweezer (1064 nm). The green color is from an optical pump 532 nm laser. The trapping lens is on the left, and the lens on the right is used to collimate the light exiting the trap. Figure adopted from ref. [49]. Image credit: J. Adam Fenster, University of Rochester.

Here we discuss some new directions and ideas in the field. Up to now, we have only considered the first order magnetic gradient induced coupling. It would be interesting to study second order gradient induced spin-resonator coupling. This coupling mechanism may have some new applications and features. For example, it may be used to entangle NV centers with different transition frequencies. It may also be used for cooling the mechanical resonator, which is out of Lamb-Dicke regime.

Another new direction is to study the coupling between rotation degree of freedom of trapped nano-diamond to the internal NV centers electron spins. Geometric phase, even non-Abelian geometric phase may be induced by mechanical rotation [72,73]. The rotation may also be cooled and manipulated by NV centers.

It would be interesting to investigate how to cool down the internal temperature of the diamond, which hosts the NV centers. As we know, the decay rate of the NV centers electron spins is inversely proportional to the temperature. Only under the low temperature $T < 10$ K, the decay rate can be decreased to around Hz. By considering the coupling between NV center electron spins and the phonons in the diamond, it would be actively cooled down to the temperature of a nano-diamond trapped with an optical tweezers [74, 75]. In this way, we may extend the lifetime of NV centers electron spins around second even at room temperature environment.

Before conclusion, we note that the proposals and schemes discussed in this review should also be applied in other similar systems, such as hybrid mechanical resonator with quantum dots [76], ^{2}8Si nanoparticles with donor spins [77], or nanocrystals doped with rare-earth ions [78].

This work was supported by the National Basic Research Program of China (Grant Nos. 2011CBA00300 and 2011CBA00302), the National Natural Science Foundation of China (Grant Nos. 11105136, 61435007, 11374032 and 11121403) and the National Key Basic Research Program of China (Grant No. 2014CB848700). LI TongGang acknowledges the support given by Purdue University through the startup fund.

1 Wieman C E, Pritchard D E, Wineland D J. Atom cooling, trapping, and quantum manipulation. Rev Mod Phys, 1999, 71: S253–S262
2 Wineland D J. Nobel Lecture: Superposition, entanglement, and raising Schrödingers cat. Rev Mod Phys, 2013, 85: 1103–1114
3 Monroe C, Meekhof D M, King B E, et al. A Schrödinger cat superposition state of an atom. Science, 1996, 272(5265): 1131–1136
4 Einstein A. On the development of our views concerning the nature and constitution of radiation. Physica Z, 1909, 10: 817
5 Braginski V B, Manukin A B. Ponderomotive effects of electromagnetic radiation. Sov Phys-JETP, 1967, 25: 653–655
6 Ashkin A. Acceleration and trapping of particles by radiation pressure. Phys Rev Lett, 1970, 24: 156–159
7 Ashkin A, Dziedzic J M. Optical levitation by radiation pressure. Appl Phys Lett, 1971, 19: 283–285
8 Aspelmeyer M, Meystre P, Schwab K. Quantum optomechanics. Phys Tod, 2012, 65: 29–35
9 Aspelmeyer M, Kippenberg T J, Marquardt F. Cavity optomechanics. Rev Mod Phys, 2014, 86: 1391
10 Liu Y C, Hu Y W, Wong C W, et al. Review of cavity optomechanical cooling. Chin Phys B, 2013, 22: 114213
11 OConnell A D, Hofheinz M, Ansmann M, et al. Quantum ground state and single-phonon control of a mechanical resonator. Nature, 2010, 464: 697–703
12 Teufel J D, Donner T, Li D, et al. Sideband cooling of micromechanical motion to the quantum ground state. Nature, 2011, 475: 359–363
13 Chan J, Alegre T P M, Safavi-Naeini A H, et al. Laser cooling of a nanomechanical oscillator into its quantum ground state. Nature, 2011, 478: 89–92
14 Verhagen E, Deléglise S, Weis S, et al. Quantum-coherent coupling of a mechanical oscillator to an optical cavity mode. Nature, 2012, 482(7383): 63–67
15 Weis S, Riviére R, Deléglise S, et al. Optomechanically induced transparency. Science, 2010, 330: 1520–1523
16 Dong C H, Shen Z, Zou C L, et al. Interconversion of photon-phonon in a silica optomechanical microresonator. Sci China-Phys Mech Astron, 2015, 58: 050308
17 Liu Y-C, Xiao Y-F, Luan X S, et al. Optomechanically-induced-transparency cooling of massive mechanical resonators to the quantum ground state. Sci China-Phys Mech Astron, 2015, 58: 050305
18 Purdy T P, Yu P L, Peterson R W, et al. Strong optomechanical squeezing of light. Phys Rev X, 2013, 3: 031012
19 Wang Y D, Clerk A A. Using interference for high fidelity quantum state transfer in optomechanics. Phys Rev Lett, 2012, 108: 153603
20 Andrews R W, Peterson R W, Purdy T P, et al. Bidirectional and efficient conversion between microwave and optical light. Nat Phys, 2014, 10: 321–326
21 Yin Z, Yang W L, Sun L, et al. Quantum network of superconducting qubits through opto-mechanical interface. Phys Rev A, 2015, 91: 012333
22 Romero-Isart O, Pflanzer A C, Blaser F, et al. Large quantum superpositions and interference of massive nanometer-sized objects. Phys Review Lett, 2011, 107: 020405
23 Romero-Isart O, Juan M L, Quidant R, et al. Toward quantum superposition of living organisms. New J Phys, 2010, 12: 033015
24 Penrose R. On gravity's role in quantum state reduction. General Relativity Gravitation, 1996, 28: 581–600
25 Ghirardi G C, Rimini A, Weber T. Unified dynamics for microscopic and macroscopic systems. Phys Rev D, 1986, 34: 470–491
26 Ghirardi G C, Pearle P, Rimini A. Markov processes in Hilbert space and continuous spontaneous localization of systems of identical particles. Phys Rev A, 1990, 42: 78–89
27 Xiong H, Si L G, Lü X Y, et al. Review of cavity optomechanics in the weak-coupling regime: From linearization to intrinsic nonlinear interactions. Sci China-Phys Mech Astron, 2015, 58: 050302
28 Wilson-Rae I, Zoller P, Imamoḡlu A. Laser cooling of a nanomechanical resonator mode to its quantum ground state. Phys Rev Lett, 2004, 92: 075507
29 Bennett S D, Cockins L, Miyahara Y, et al. Strong electromechanical coupling of an atomic force microscope cantilever to a quantum dot. Phys Rev Lett, 2010, 104: 017203
30 Hammerer K, Wallquist M, Genes C, et al. Strong coupling of a mechanical oscillator and a single atom. Phys Rev Lett, 2009, 103: 063005
31 Rabl P, Cappellaro P, Dutt M V G, et al. Strong magnetic coupling between an electronic spin qubit and a mechanical resonator. Phys Rev B, 2009, 79: 041302
32 Rabl P, Kolkowitz S J, Koppens F H L, et al. A quantum spin transducer based on nanoelectromechanical resonator arrays. Nat Phys, 2010, 6: 602–608
33 Arcizet O, Jacques V, Siria A, et al. A single nitrogen-vacancy defect

coupled to a nanomechanical oscillator. Nat Phys, 2011, 7: 879–883
34 Kolkowitz S, Jayich A C B, Unterreithmeier Q P, et al. Coherent sensing of a mechanical resonator with a single-spin qubit. Science, 2012, 335: 1603–1606
35 Bar-Gill N, Pham L M, Belthangady C, et al. Suppression of spin-bath dynamics for improved coherence of multi-spin-qubit systems. Nat Commun, 2012, 3: 858
36 Balasubramanian G, Neumann P, Twitchen D, et al. Ultralong spin coherence time in isotopically engineered diamond. Nat Mater, 2009, 8: 383–387
37 Zhao N, Honert J, Schmid B, et al. Sensing single remote nuclear spins. Nat Nanotech, 2012, 7: 657–662
38 Shi F, Kong X, Wang P, et al. Sensing and atomic-scale structure analysis of single nuclear-spin clusters in diamond. Nat Phys, 2014, 10: 21–25
39 Bennett S D, Yao N Y, Otterbach J, et al. Phonon-induced spin-spin interactions in diamond nanostructures: Application to spin squeezing. Phys Rev Lett, 2013, 110: 156402
40 Zhang J Q, Zhang S, Zou J H, et al. Fast optical cooling of nanomechanical cantilever with the dynamical Zeeman effect. Opt Express, 2013, 21: 29695–29710
41 Kepesidis K V, Bennett S D, Portolan S, et al. Phonon cooling and lasing with nitrogen-vacancy centers in diamond. Phy Rev B, 2013, 88(6): 064105
42 Zwickl B M, Shanks W E, Jayich A M, et al. High quality mechanical and optical properties of commercial silicon nitride membranes. Appl Phys Lett, 2008, 92: 103125
43 Chang D E, Regal C A, Papp S B, et al. Cavity opto-mechanics using an optically levitated nanosphere. PNAS, 2010, 107: 1005–1010
44 Li T, Kheifets S, Raizen M G. Millikelvin cooling of an optically trapped microsphere in vacuum. Nat Phys, 2011, 7: 527–530
45 Gieseler J, Deutsch B, Quidant R, et al. Subkelvin parametric feedback cooling of a laser-trapped nanoparticle. Phys Rev Lett, 2012, 109: 103603
46 Yin Z, Li T, Feng M. Three-dimensional cooling and detection of a nanosphere with a single cavity. Phys Rev A, 2011, 83: 013816
47 Kiesel N, Blaser F, Delić U, et al. Cavity cooling of an optically levitated submicron particle. PNAS, 2013, 110: 14180–14185
48 Yin Z, Geraci A A, Li T. Optomechanics of levitated dielectric particles. Int J Mod Phys B, 2013, 27: 1330018
49 Neukirch L P, Vamivakas A N. Nano-optomechanics with optically levitated nanoparticles. Contemporary Phys, 2014, Doi: 10.1080/00107514.2014.969492
50 Nie W, Lan Y, Li Y, et al. Dynamics of a levitated nanosphere by optomechanical coupling and Casimir interaction. Phys Rev A, 2013, 88: 063849
51 Nie W J, Lan Y H, Li Y, et al. Generating large steady-state optomechanical entanglement by the action of Casimir force. Sci China-Phys Mech Astron, 2014, 57: 2276–2284
52 Liu Y C, Liu R S, Dong C H, et al. Cooling mechanical resonators to quantum ground state from room temperature. Phys Rev A, 2014, 91: 013824
53 Yin Z, Li T, Zhang X, et al. Large quantum superpositions of a levitated nanodiamond through spin-optomechanical coupling. Phys Rev A, 2013, 88: 033614
54 Neukirch L P, Gieseler J, Quidant R, et al. Observation of nitrogen vacancy photoluminescence from an optically levitated nanodiamond. Opt Lett, 2013, 38: 2976–2979
55 Scala M, Kim M S, Morley G W, et al. Matter-wave interferometry of a levitated thermal nano-oscillator induced and probed by a spin. Phys Rev Lett, 2013, 111: 180403
56 Asadian A, Brukner C, Rabl P. Probing macroscopic realism via ramsey correlation measurements. Phys Rev Lett, 2014, 112: 190402
57 Zhao N, Yin Z. Room-temperature ultra-sensitive mass spectrometer via dynamic decoupling. Phys Rev A, 2013, 90: 042118
58 Rabl P. Cooling of mechanical motion with a two-level system: The high-temperature regime. Phys Rev B, 2010, 82: 165320
59 Zhou L, Wei L F, Gao M, et al. Strong coupling between two distant electronic spins via a nanomechanical resonator. Phys Rev A, 2010, 81: 042323
60 Xu Z Y, Hu Y M, Yang W L, et al. Deterministically entangling distant nitrogen-vacancy centers by a nanomechanical cantilever. Phys Rev A, 2009, 80: 022335
61 Chen Q, Xu Z, Feng M. Entanglement generation of nitrogen-vacancy centers via coupling to nanometer-sized resonators and a superconducting interference device. Phys Rev A, 2010, 82: 014302
62 Zheng S B, Guo G C. Efficient scheme for two-atom entanglement and quantum information processing in cavity QED. Phys Rev Lett, 2000, 85: 2392–2395
63 Doherty M W, Dolde F, Fedder H, et al. Theory of the ground-state spin of the NV-center in diamond. Phys Rev B, 2012, 85: 205203
64 Dolde F, Fedder H, Doherty M W, et al. Electric-field sensing using single diamond spins. Nat Phys, 2011, 7: 459–463
65 Teissier J, Barfuss A, Appel P, et al. Strain coupling of a nitrogen-vacancy center spin to a diamond mechanical oscillator. Phys Rev Lett, 2014, 113: 020503
66 Ma J, Wang X, Sun C P, et al. Quantum spin squeezing. Phys Rep, 2011, 509: 89–165
67 Robledo L, Childress L, Bernien H, et al. High-fidelity projective readout of a solid-state spin quantum register. Nature, 2011, 477: 574–578
68 Tsang C, Bonhote C, Dai Q, et al. Head challenges for perpendicular recording at high areal density. IEEE Trans Magn, 2006, 42: 145–150
69 Mamin H J, Poggio M, Degen C L, et al. Nuclear magnetic resonance imaging with 90-nm resolution. Nat Nanotech, 2007, 2: 301–306
70 Chen X, Ruschhaupt A, Schmidt S, et al. Fast optimal frictionless atom cooling in harmonic traps: Shortcut to adiabaticity. Phys Rev Lett, 2010, 104: 063002
71 Kuhlicke A, Schell A W, Zoll J, et al. Nitrogen vacancy center fluorescence from a submicron diamond cluster levitated in a linear quadrupole ion trap. Appl Phys Lett, 2014, 105: 073101
72 Maclaurin D, Doherty M W, Hollenberg L C L, et al. Measurable quantum geometric phase from a rotating single spin. Phys Rev Lett, 2012, 108: 240403
73 Kowarsky M A, Hollenberg L C L, Martin A M. Non-Abelian geometric phase in the diamond nitrogen-vacancy center. Phys Rev A, 2014 90: 042116
74 Seletskiy D V, Melgaard S D, Bigotta S, et al. Laser cooling of solids to cryogenic temperatures. Nat Photon, 2010, 4: 161–164
75 Zhang J, Li D, Chen R, et al. Laser cooling of a semiconductor by 40 kelvin. Nature, 2013, 493: 504–508
76 Bell D M, Howder C R, Johnson R C, et al. Single CdSe/ZnS nanocrystals in an ion trap: Charge and mass determination and photophysics evolution with changing mass, charge, and temperature. ACS Nano, 2014, 8: 2387–2398
77 Steger M, Saeedi K, Thewalt M L W, et al. Quantum information storage for over 180 s using donor spins in a 28Si "semiconductor vacuum". Science, 2012, 336: 1280–1283
78 Afzelius M, Chaneliére T, Cone R L, et al. Photon-echo quantum memory in solid state systems. Laser Photon Rev, 2010, 4: 244–267